Weak Interaction Processes
in Core-Collapse Supernovae

G. Martínez-Pinedo[1,2], K. Langanke[3], J.M. Sampaio[3], D.J. Dean[4],
W.R. Hix[4,5,6], O.E.B. Messer[4,5,6], A. Mezzacappa[4], M. Liebendorfer[7,4,5],
H.-Th. Janka[8], and M. Rampp[8]

[1] Institut d'Estudis Espacials de Catalunya, Barcelona, Spain;
    martinez@ieec.fcr.es
[2] Institució Catalana de Recerca i Estudis Avançats, Barcelona, Spain
[3] Institute for Physics and Astronomy, University of Århus, Denmark
[4] Physics Division, Oak Ridge National Laboratory, Tennessee, USA
[5] Department of Physics and Astronomy, University of Tennessee, USA
[6] Joint Institute for Heavy Ion research, Oak Ridge, Tennessee, USA
[7] Canadian Institute for Theoretical Astrophysics, Toronto, Ontario, Canada
[8] Max-Planck-Institut fur Astrophysik, Garching, Germany

Summary. Supernova simulations to date have assumed that during core collapse electron captures (EC) occur dominantly on free protons, while captures on heavy nuclei are Pauli-blocked and are ignored. Using microscopic calculations we show that the EC rates on heavy nuclei are large enough that, in contrast to previous assumptions, electron capture on nuclei dominates over capture on free protons. This leads to significant changes in core collapse simulations.

1 Introduction

Stars with masses exceeding roughly 10 $M_\odot$ reach a moment in their evolution when their iron core provides no further source of nuclear energy generation. At this time, the evolution in the core is determined by the competition of gravity, that produces the collapse of the core, and the weak interaction, that determines the rate at which electrons are captured and the rate at which neutrinos are trapped during the collapse. As the density of the star's center increases electrons become more degenerate and their chemical potential grows. For sufficiently high values of the chemical potential electrons are captured by nuclei producing neutrinos, which for densities $\lesssim 10^{11}$ g cm^{-3}, freely escape from the star, removing energy and entropy from the core. Thus entropy stays low during the collapse ensuring that nuclei dominate in the composition over free nucleons.

Before the collapse sets in, during the presupernova stage, i.e. at core densities $\lesssim 10^{10}$ g cm^{-3}, and proton-to-neutron ratios $Y_e \gtrsim 0.42$, nuclei with $A = 55 - 65$ dominate in the composition. The relevant rates for weak interaction processes were initially determined by Fuller, Fowler and Newman [4]. The rates have been recently improved based on modern data and state-of-
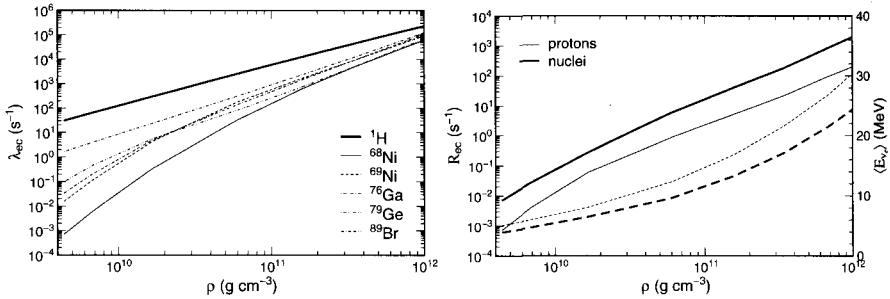
Fig. 1. (left panel) Comparison of the electron capture rates on free protons and selected nuclei as function of the electron chemical potential along a stellar collapse trajectory. (right panel) The reaction rates for electron capture on protons (thin line) and nuclei (thick line) are compared as a function of density along a stellar collapse trajectory. The dashed lines (right scale) show the related average energy of the neutrinos emitted by capture on nuclei and protons.

the-art shell-model calculations [13, 14]. Presupernova models utilizing these improved weak rates are presented in [9, 10].

During collapse, i.e., at densities $\gtrsim 10^{10}$ g cm^{-3}, temperatures and densities are high enough to ensure that nuclear statistical equilibrium is achieved. Then, for sufficiently low entropies, the matter composition is dominated by the nuclei with the largest binding energy for a given Y_e. In current collapse simulations a very simple description of electron capture on nuclei is used. The rates are estimated using an independent particle model (IPM) that assumes pure Gamow-Teller (GT) transitions [2]. In this model GT transitions are Pauli-blocked for nuclei with $N \geq 40$ and $Z \leq 40$ [5, 6]. These nuclei dominate the composition for densities larger than a few 10^{10} g cm^{-3}. As a result, electron capture on nuclei ceases at these densities and the capture is entirely due to free protons. In the next section we will show that the employed model for electron capture on nuclei is incorrect, as Pauli-blocking of the GT transitions is overcome once correlations [15] and temperature effects are taken in account [3, 5, 6].

2 Electron Capture During Core Collapse

The residual nuclear interaction, beyond the IPM, mixes the pf shell with the levels of the sdg shell, in particular, with the lowest orbital, $g_{9/2}$. The presence of configurations were more than a neutron is promoted from the pf shell into the $g_{9/2}$ orbit unblocks the GT transitions for nuclei with $N \geq 40$. In addition, during core collapse electron capture occurs at temperatures $T \gtrsim 0.8$ MeV. A model that is a able to describe both correlations and finite temperature is then necessary for the calculation of the relevant rates. This model is the
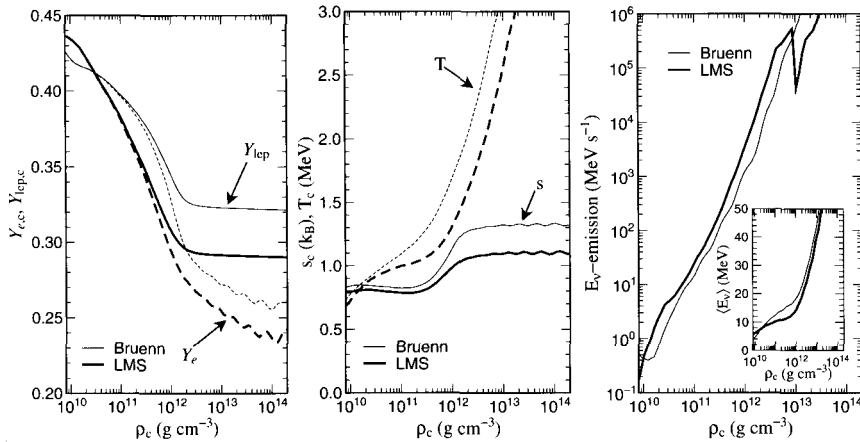
Fig. 2. Comparison of the evolution of several quantities at the center of a 15 $M_\odot$. The initial presupernova model was taken from [9, 10]. The thin line is a simulation using the Bruenn parameterization [2] while the thick line uses the LMS rate set (see text). Both models were calculated using a General Relativistic treatment of gravity by the Garching collaboration.

shell model Monte Carlo (SMMC) [12] supplemented with calculations based in the random phase approximation for the transition operators [16].

The left panel of Fig. 1 shows the electron capture rates for protons and selected nuclei along a stellar trajectory taken from [18]. The electron chemical potential, μ_e, and the reaction Q value are the two important energy scales of the capture process. For the lowest densities the electron chemical potential ($\mu_e \approx 6$ MeV for $\rho = 5 \times 10^9$ g cm^{-3}) is of the same order than the typical nuclear Q value. Then, the electron capture rates on nuclei are very sensitive to the Q-value and smaller than the rate on protons. For higher densities the chemical potential grows much faster than the Q-value and the rate becomes independent of the heavy nucleus. Due to the much smaller Q-value, the electron capture rate on free protons is larger than the rates on the abundant nuclei during the collapse. However, this is misleading as the low entropy keeps the protons significantly less abundant than heavy nuclei. The right panel of Fig. 1 shows that the reaction rate for electron capture on heavy nuclei ($R_h = \sum_i Y_i \lambda_i$, where the sum runs over all the nuclei present and Y_i denotes the number abundance of species i) dominates over the one of protons ($R_p = Y_p \lambda_p$) by roughly an order of magnitude throughout the collapse, when the composition is considered.

Electron capture on nuclei and on free protons differ quite noticeably in the neutrino spectra they generate. The right panel of Fig. 1 shows that neutrinos produced by captures on nuclei have a mean energy 40–60% smaller than those produced by captures on protons (mainly due to the larger Q-value for capture on nuclei). Despite that, the total neutrino energy loss rate

is larger when electron capture on nuclei is considered, caused by the increase in the total (nuclei plus protons) electron capture rate.

3 Consequences for the Collapse

Simulations of core collapse require reaction rates for the electron capture on protons, R_p, and heavy nuclei, R_h. While R_p is readily derived from [2], the calculation of R_h requires knowledge of the nuclear composition, in addition to the electron capture rates described earlier. In order to compute the needed abundances a Saha-like nuclear statistical equilibrium (NSE) is used to calculate the needed abundances of individual isotopes, including coulomb corrections to the nuclear binding energy [1, 11]. Coulomb corrections to the electron capture rates themselves impose a reduction of a factor ~ 2, that doesn't produce appreciable differences with the results obtained using unscreened rates that are discussed below [17]. The combination of NSE abundances with electron capture rates for around 200 nuclei with $A = 45$–112 was used [16] to compute the rate of electron capture on nuclei and the emitted neutrino spectra as a function of temperature, density, and electron fraction, adequately covering the range until weak equilibrium during the collapse is achieved. The range of validity is estimated to be $\rho \lesssim 2 \times 10^{12}$ g cm^{-3} and $T \lesssim 2$ MeV. This rate set will be denoted LMS (Langanke, Martínez-Pinedo, and Sampaio) in the following. The rates for the inverse neutrino absorption process are determined by detailed balance.

The consequences of this more realistic implementation of electron capture rates on heavy nuclei have been evaluated in independent self-consistent neutrino radiation hydrodynamics simulations by the Oak Ridge and Garching Collaborations. The basis of these models is described in detail in [18, 19]. The results obtained by the Garching collaboration for the evolution of several quantities at the center of a 15 $M_\odot$ star using the standard treatment of Bruenn [2] and the new LMS rates for heavy nuclei are compared in Fig. 2. With the improved treatment of electron capture rate on heavy nuclei the total electron capture rate (heavy nuclei plus protons) is bigger than in the Bruenn treatment resulting in a smaller Y_e value and Y_{lepton}. The right panel shows that the energy emission rate by neutrinos is higher in the LMS treatment resulting in a reduction of the central temperature and entropy (middle panel). Notice however, that the average energy of the emitted neutrinos is smaller in the LMS treatment due to the higher Q-values for electron capture on nuclei (inset of the right panel).

Figure 3 shows the star profiles for several quantities obtained in collapse simulations carried out by the Oak Ridge collaboration (similar results are obtained by the Garching collaboration) at the moment when the central density reaches 10^{14} g cm^{-3}. In the inner regions of the star, the additional electron capture on heavy nuclei results in more electron capture in the LMS models that produce a reduction in Y_e and a smaller central temperature.
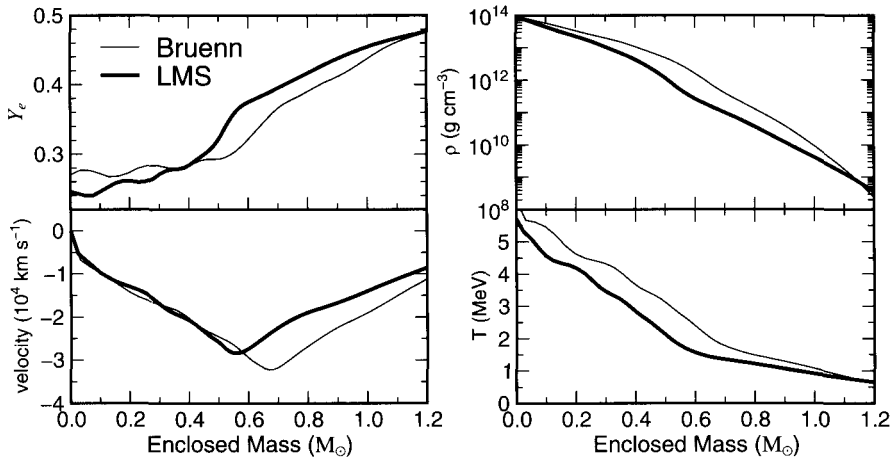
Fig. 3. The electron fraction, velocity, density and temperature as functions of the enclosed mass at the moment when the center reaches nuclear matter densities for the same 15 M$_\odot$ star as Fig. 2. The thin line is a simulation using the Bruenn parameterization [2] while the thick line uses the LMS rate set (see text). Both models were calculated using Newtonian gravity by the Oak Ridge collaboration.

In outer regions, where $A < 65$ nuclei dominate, the LMS models predict less electron capture. This is so, because for these mass ranges the electron capture rates of ref. [13, 14] are smaller than the ones used in the Bruenn parameterization [2]. Due to the smaller electron capture rates, these regions collapse more slowly so that the density and temperature are smaller in the new models. The velocity distribution shows a displacement in the minimum, which marks the eventual location of shock formation, by 0.1 M$_\odot$.

References

1. E. Bravo, D. García-Senz: Mon. Not. R. Astron. Soc. **307**, 984 (1999)
2. S.W. Bruenn: Astrophys. J. Suppl. **58**, 771 (1985)
3. J. Cooperstein, J. Wambach: Nuc. Phys. **420**, 591 (1984)
4. G.M. Fuller, W.A. Fowler, M.J. Newman: Astrophys. J. Suppl. **42**, 447 (1980)
5. G.M. Fuller, W.A. Fowler, M.J. Newman: Astrophys. J. Suppl. **48**, 279 (1982)
6. G.M. Fuller, W.A. Fowler, M.J. Newman: Astrophys. J. **252**, 715 (1982)
7. G.M. Fuller: Astrophys. J. **252**, 741 (1982)
8. G.M. Fuller, W.A. Fowler, M.J. Newman: Astrophys. J. **293**, 1 (1985)
9. A. Heger, K. Langanke, G. Martínez-Pinedo, S.E. Woosley: Phys. Rev. Lett. **86**, 1678 (2001)

10. A. Heger, K. Langanke, G. Martínez-Pinedo, S.E. Woosley: Astrophys. J. **560**, 307 (2001)
11. W.R. Hix: Ph.D. Thesis (Harvard Univ.: 1995)
12. S.E. Koonin, D.J. Dean, K. Langanke: Phys. Rep. **278**, 2 (1997)
13. K. Langanke, G. Martínez-Pinedo: Nuc. Phys. **673**, 481 (2000)
14. K. Langanke, G. Martínez-Pinedo: At. Data. Nucl. Data Tables **79**, 1 (2001)
15. K. Langanke, E. Kolbe, D.J. Dean: Phys. Rev. C **63**, 032801 (2001)
16. K. Langanke etal.: Phys. Rev. Lett. **90**, 241102 (2003)
17. G. Martínez-Pinedo, K. Langanke, H.-T. Janka, M. Rampp: in preparation
18. A. Mezzacappa etal.: Phys. Rev. Lett. **86**, 1935 (2001)
19. M. Rampp, H.-T. Janka: Astron. Astrophys. **396**, 361 (2002)